Gross et al., *"Antitumor Activity of the Glutaminase Inhibitor CB-839 in TNBC"*

Supplementary Materials and Methods

Biochemical glutaminase assay

N-terminally truncated recombinant human GAC (rHu-GAC; amino acids 126-598; accession NP_001243239) with a His_6-tag was expressed in E. coli and purified by column chromatography (Ni affinity capture and gel filtration). The enzymatic activity was measured in assay buffer containing 50 mM Tris-Acetate pH 8.6, 150 mM K_2HPO_4, 0.25 mM EDTA, 0.1 mg/ml bovine serum albumin (BSA) (Calbiochem), 1 mM DTT, 2 mM NADP+ (Sigma Aldrich) and 0.01% Triton X-100. To measure inhibition, the inhibitor (prepared in DMSO) was first pre-mixed with glutamine and glutamate dehydrogenase (GDH) (Sigma Aldrich) and reactions were initiated by the addition of rHu-GAC. Final reactions contained 2 nM rHu-GAC, 10 mM glutamine, 6 units/mL GDH and 2% DMSO. Generation of NADPH was monitored by fluorescence (Ex340/Em460 nm) every minute for 15 minutes on a SpectraMax M5e plate reader (Molecular Devices at 25°C. Relative fluorescence units (RFU) were converted to units of NADPH concentration (μM) using a standard curve of NADPH. Each assay plate incorporated control reactions that monitored the conversion of glutamate (1 to 75 μM) plus NADP+ to α-ketoglutarate plus NADPH by GDH. Under these assay conditions, up to 75 μM glutamate is stoichiometrically converted to α-ketoglutarate/NADPH by GDH. Initial reaction velocities were calculated by fitting the first 5 minutes of each progress curve to a straight line. Inhibition curves were fitted (GraphPad Prism) to a four-parameter dose response equation of the form: % activity = Bottom + (Top-Bottom)/(1+10^((LogIC50-X)*HillSlope)).

Preparation of homogenates from cell lines and tissues

Tissues were freshly excised from healthy female CD-1 mice. Tumors were excised from tumor-bearing female Scid/Bg mice implanted in the mammary fat pad. Tissues or tumors were cut into pieces weighing between 50 and 75 mg and snap frozen in liquid nitrogen. On the day of homogenate preparation, tissues were thawed and ten volumes of ice-cold homogenization buffer [10 mM Tris-Acetate pH 8.6, 100 mM K_2HPO_4, 1X complete protease inhibitors (Roche)] was added. A single refrigerated steel bead (Qiagen) was added to each tube and samples were subjected to two rounds of homogenization on a Tissue Lyser II (Qiagen) for 1 minute per cycle at a frequency of 20 Hz. The homogenates were clarified by centrifugation (10 minutes, 4°C, 18,000 x g). The supernatant was

adjusted to 5% (v/v) glycerol and passed over a gel filtration spin column (Zeba Spin Desalting Column, Thermo) pre-equilibrated in homogenization buffer containing 5% (v/v) glycerol. Gel filtered homogenates were quantified for total protein (Pierce), snap frozen in liquid nitrogen, and stored at -80 °C. Homogenates were prepared from tumor cell line pellets (10-20 million cells per pellet) by sonication in 250 µL of cell homogenization buffer (50 mM Tris-Acetate pH 8.6, 150 mM K_2HPO_4, 0.25 mM EDTA, 1 mM DTT, 1X complete protease inhibitors) using a Bioruptor sonication device (Diagenode) for 5 minutes at 4 °C on high power (30 sec on/30 sec off per 1 minute cycle). The homogenates were gel filtered as described above, except spin columns were equilibrated in cell homogenization buffer supplemented with 0.01% Triton X-100.

When measuring glutaminase activity in the homogenates, the background activity that is independent of glutaminase was measured from reactions that lacked glutamine. Background activity was subtracted from activity measured in the presence of glutamine. The specific activity of glutaminase was calculated by dividing the background-subtracted glutaminase activity by the total protein amount present in the reaction.

Western blot validation

To validate the identity and mobility of the glutaminase splice variants (KGA and GAC) detected with the dual-specificity antibody used in Figure 3A, we evaluated independent antibody preparations specific for either KGA or GAC. We resolved MCF10A cell lysate (a cell line that expresses both KGA and GAC) next to recombinant GAC (ΔN-GAC, residues 126-598 plus two N-terminal residues left after TEV protease cleavage, calculated molecular mass 52911 Daltons) next to recombinant KGA (ΔN-KGA, residues 126-669 plus two N-terminal residues left after TEV protease cleavage, calculated molecular mass 60912 Daltons) on three sets of adjacent lanes on a single gel under conditions identical to those in Fig. 3A (7% Tris/Acetate gels, Novex Sharp pre-stained molecular weight standards), transferred the proteins to nitrocellulose, cut the blot into three identical strips, and probed with three different antibodies: 1) a KGA-specific antibody that recognizes the unique C-terminal tail of KGA (a gift from Dr. N. Curthoys, Colorado State University); 2) a commercial GAC-specific antibody that recognizes the unique C-terminal tail of GAC (Proteintech Group, #19958-1-AP); and 3) the antibody used for Figure 3A, a commercial GAC/KGA dual-specificity antibody (Abcam, #ab156876) that recognizes an epitope within the N-terminal region (between amino acids 72 and 125) that is common to both endogenous GAC and KGA, but is not present in either ΔN-GAC or ΔN-KGA.

These blots (see image below) demonstrate that both the KGA-specific and the GAC/KGA dual-specificity antibodies detect a major band in MCF10A lysate that runs slightly below the 60 kDa marker. As expected, ΔN-KGA is detected by the KGA-specific antibody (with a lower-than-calculated apparent molecular mass of ~54 kDa) but not the KGA/GAC dual-specificity antibody, while neither antibody detects ΔN-GAC. Conversely, the GAC-specific antibody and the GAC/KGA dual-specificity antibody both detect a major band in MCF10A lysate that runs between the 60 kDa and 50 kDa markers. ΔN-GAC is detected by the GAC-specific antibody (with a lower-than-calculated apparent molecular mass of ~50 kDa) but not the KGA/GAC dual-specificity antibody, while neither antibody detects ΔN-KGA. These data demonstrate that two independent antibodies are each capable of detecting a protein in MCF10A lysate of precisely the same apparent molecular weight and with the predicted selectivity between the GAC and KGA isoforms.

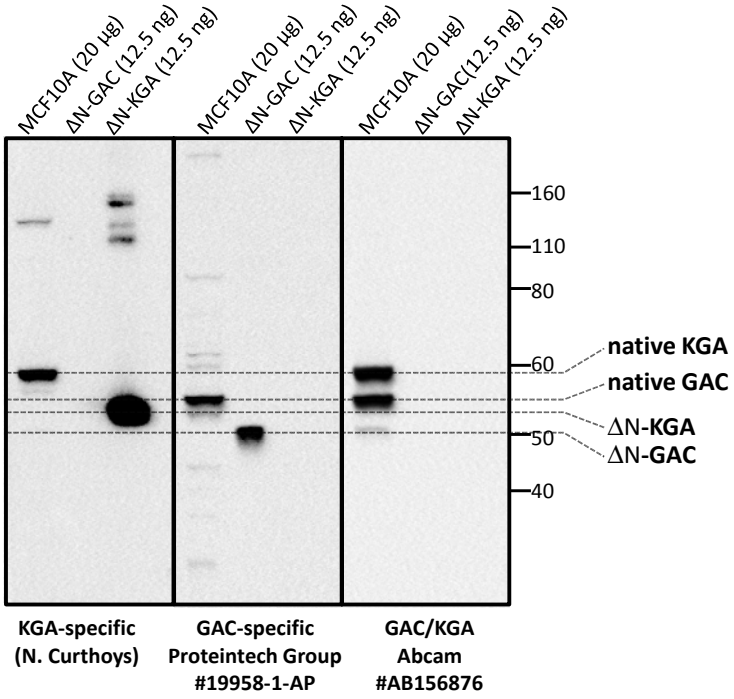

This data provides evidence that endogenous KGA and GAC migrate with apparent molecular weights of ~60 kDa and ~55 kDa under these conditions (somewhat smaller than predicted) and validate the results obtained with the KGA/GAC dual-specificity antibody.

Gene expression qnalysis

IlluminaHiSeq expression datasets (gene-level and exon-level) from the The Cancer Genome Atlas (TCGA) breast invasive carcinoma collection (1) were downloaded from the UCSC Cancer Genomics Browser (https://genome-cancer.soe.ucsc.edu). The gene-level dataset (log2 transformed RSEM normalized counts) was evaluated for expression of glutamine synthetase (*GLUL*) and *GLS2*; the exon-level dataset (log2 transformed RPKM values) was evaluated for expression of the *GAC* and *KGA* splice variants of *GLS*. The annotated hormone receptor and HER2 status based on clinical histopathological

evaluation was used to assign the samples into receptor positive (N=584; comprised of 475 ER+/HER2-, 31 ER-/HER2+, and 78 ER+/HER2+) and TNBC (N=132) categories. An additional set of normal breast tissue (N=107) from the TCGA dataset was included in the analysis. Statistical comparisons between tumor subsets and normal tissue were done by one-way ANOVA. A similar analysis was done on the expression data for the 58 breast cancer cell lines listed in The Cancer Cell Line Encyclopedia (CCLE) (2). Expression levels (log2 transformed RMA normalized values) for *KGA* (probeset 203159_at), *GAC* (probeset 221510_s_at), *GLUL* (probeset 215001_s_at), and *GLS2* (probeset 205531_s_at) were evaluated. Since this dataset was not annotated with receptor status, the ER and HER2 status was assigned based on the distribution mRNA expression levels for ER+ (*ESR*) and HER2 (*ERBB2*) across the cell line panel. Based on this analysis, cell lines were classified as TNBC (N=31) or receptor-positive (N=27; comprised of 13 ER+/HER2-, 7 ER-/HER2+, and 7 ER+/HER2+). There was good concordance between the receptor status assigned by this method and that described for a panel of 54 breast cancer cell lines (3) with 32 out of the 33 cell lines present in both collections having the same classification. Statistical comparisons between TNBC and receptor-positive subtypes were performed by unpaired t-test .

Cell counting, apoptosis assay, and cell cycle analysis

HCC1806, JIMT-1, and MDA-MB-231 cells were treated with a dose range of CB-839 for 72 h at 37°C with 5% CO_2. Anti-proliferative effects were determined by measuring ATP levels using Cell Titer Glo reagent (Promega) and by cell counting using the Guava Viacount Reagent (Millipore) following the manufactures' instructions. The Cell Titer Glo signal and cell counts were measured on the day of compound addition and compared to the measurements taken at 72 h to determine effects on cell growth and survival during the assay period. Inhibition curves were fitted (GraphPad Prism) to a four-parameter dose response equation of the form: % activity = Bottom + (Top-Bottom)/(1+10^((LogIC50-X)*HillSlope)). Caspase induction following treatment with 1 µM CB-839 for 72 h was monitored using Caspase 3/7 Glo (Promega). Signals measured at 72 h were normalized to the cell number per well to calculate the Caspase/Glo signal per cell.

Rescue experiments

MDA-MB-231, HCC1806 and JIMT-1 cell lines were seeded in 96 well plates and treated with 1 µM CB-839 in the presence or absence of 1 mM (MDA-MB-231 only) or 4 mM dimethyl alpha-ketoglutarate (Sigma-Aldrich), 4 mM oxaloacetate (OAA; Sigma-Aldrich), 4 mM glutathione reduced ethyl ester (GSH-

MEE) (Sigma-Aldrich), or the combination of OAA and GSH-MEE (both at 4 mM). Cells were incubated for 72 h at 37°C with 5% CO_2 and analyzed for anti-proliferative effects using Cell Titer Glo (Promega).

Reference List

(1) Cancer Genome Atlas Network. Comprehensive molecular portraits of human breast tumours. Nature 2012;490:61-70.

(2) Barretina J, Caponigro G, Stransky N, Venkatesan K, Margolin AA, Kim S, et al. The Cancer Cell Line Encyclopedia enables predictive modelling of anticancer drug sensitivity. Nature 2012;483:603-7.

(3) Neve RM, Chin K, Fridlyand J, Yeh J, Baehner FL, Fevr T, et al. A collection of breast cancer cell lines for the study of functionally distinct cancer subtypes. Cancer Cell 2006;10:515-27.